APPLICATION OF A SATELLITE BASED RAINFALL-RUNOFF MODEL: A CASE STUDY OF THE TRANS BOUNDARY CUVELAI BASIN IN SOUTHERN AFRICA

[a]Mufeti, P., [b]Rientjes, T.H.M., [b]Mabande, P., [b]Maathuis, B.H.P

[a]Ministry of Agriculture, Water and Forestry , Namibia Hydrological Services, Private Bag 13193 Windhoek, N/amibia

[b]Department of Water Resources, Faculty of geo-information Science and Earth Observation (ITC), Twente University, P.O.Box 6, 7500AA, Enschede, The Netherlands

Abstract

Applications of distributed hydrological models are often constrained by poor data availability. Models rely on distributed inputs for meteorological forcing and land surface parameterization. In this pilot the rainfall-runoff model LISFLOOD for large scale streamflow simulation is tested for the transboundary Cuvelai basin in Angola and Namibia. The model simulates river discharges as a function of spatial information on soils, topography and land cover. For rainfall estimation the TRMM 3B43 product has been selected whereas for evapotranspiration estimation satellite products from the LSA-SAF facility have been used. Other satellite products used are for elevation, leaf area index and land cover. Modeling focused on simulation of extreme high seasonal rainfall that caused major floodings in the area in 2009. The simulation period covered the food period (40 days). The model was manually calibrated by optimizing five parameters. Model performance was assessed by the root mean squared error and Nash Sutcliffe coefficients. Results show that simulation of an extreme event that caused major floodings is possible thus indicating the effectiveness of use of satellite based model forcing data. Also the use of satellite based land cover data proved to be effective.

1 Introduction

In 2009 large scale floods in Cuvelai basin (Namibia) caused damage of over (USD) $500 million, [1]. Intense and continuous rains throughout northern Namibia, southern Angola and western Zambia contributed to the flood. The floods led to the development of new hydrological conditions and drainage patterns as dried out lakes filled up (lake Liambezi) and fossil channels started to flow (Selinda river connecting to Kavango river), [2]. The floods caused emergency disaster conditions for one third of Namibia's population: 147 lives were lost, over 30 000 people displaced, agriculture and economic activities were disrupted, there was damage to infrastructure, and the government of Namibia declared a state of emergency [2]. Although there is an urgent need to develop adequate hydrological models to simulate and to forecast events, there is significant lack of in-situ measurements (i.e. time series) of rainfall, evapotranspiration and stream flow. This lack of data probably constitutes the biggest challenge to the development of a hydrological model that serves stream flow simulation at first but eventually should serve forecasting of impacts of extreme meteorological events. Such model also could serve for early warning. Moreover, current climate change models anticipate more frequent hydro-meteorological extremes for both droughts and floods in the decades ahead.

A post-flood investigation of the 1998 Cuvelai flood by SADC-HYCOS showed that there were no stations in operation in the part of Cuvelai basin that is located in Angola. The stream and rain gauges which were available only are very few and poorly distributed to represent the 167,400 km^2 size Namibia-Angola transboundary basin (Figure 1). Estimates of satellite based accumulated rainfall have to be assessed to better understand the spatio-temporal relationship between extreme rainfall inputs and floods. This study is an attempt to overcome the problem of data scarcity by use of satellite data, this particular for large scale and other transboundary river basins in Africa. The study aims to increase understanding of the applicability of satellite based rainfall estimation products as major inputs to rainfall-runoff models for flood simulation. We assess effectiveness of satellite products for stream flow simulation of a large area with only very little in-situ data available. This study makes part of the "ESA-Tiger capacity building in Africa" programme (http://www.tiger.esa.int/). The aim of the project is to build capacity in the field of remote sensing and hydrological modeling in this specific project.

Proc. 'ESA Living Planet Symposium 2013', Edinburgh, UK
9–13 September 2013 (ESA SP-722, December 2013)

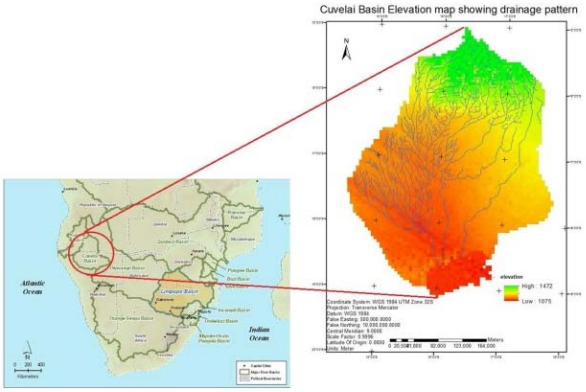

Figure 1: Location of Cuvelai Basin.

2 Satellite products

2.1 Digital elevation model (SRTM)

For representing elevation in our rainfall-runoff modeling we used the Shuttle Radar Topography Mission (SRTM) digital elevation model (DEM) with horizontal resolution of 90m at the equator. The data is projected in a Geographic (Lat/Long) projection, with the World Geodetic System 1984 (WGS84) horizontal datum and the Earth Gravitational Model of 1996 (EGM96) vertical datum [3], [4]. [4] report maximum elevation error of 16m but, given the flatness of the Cuvelai area, we anticipate only minor errors (<< 1m). The existence of regions in a DEM without data (no-data regions) can cause significant problems in using SRTM DEMs, especially in the application of distributed hydrological models. The processed DEM for the study area is available from USGS. The original acquisition contained pixels where surface water bodies and/or heavy cloud shadow prevented the accurate estimation of elevation. To overcome this problem the Consultative Group on International Agricultural Research Consortium for Spatial Information (CGIAR-CSI) SRTM data product applied a filling algorithm so to fill the data gabs. Subsequently the interpolated DEM for the no-data regions was merged with t he original DEM to provide continuous elevation surfaces without no-data regions (see [4] for a detailed description).

2.2 Rainfall estimation from space

For this study we evaluated the Multi-satellite Precipitation Analysis (TMPA 3B42) product from the Tropical Rainfall Measuring Mission (TRMM). This product is designed to combine precipitation estimates from various satellite systems and land surface precipitation from gauges. The product merges microwave (MW) infrared (IR) product and is available at 3- hourly temporal and 0.25° x 0.25° latitude–longitude spatial resolution [5]. For this study we used the post-real-time research-quality product (i.e., research product) that becomes available some fifteen days after the end of each month, [6]. The product can be downloaded from: http://gdata1.sci.gsfc.nasa.gov/daac-bin/G3/gui.cgi?instance_id=TRMM_3B42_Daily.

The research product makes use of thee independent data sources: The TRMM Combined Instrument (TCI) estimate employs data from the TRMM Microwave Imager (TMI) and the TRMM precipitation radar (PR) as source for calibration. The resulting product is the TRMM Combined Instrument (TCI) 2B31 product. The third source are the Global Precipitation Climatological Center (GPCP) monthly rain gauge analysis developed by GPCC and the Climate Assessment and Monitoring System (CAMS) monthly rain gauge analysis developed by the Climate Prediction Center (CPC) [7]. For extensive descriptions on the TMPA 3b42 product and its processing algorithm reference is made to [5], [8].

The TMPA 3B42 product algorithm V6

For estimation of rainfall intensity, passive microwave fields of view (FOVs) from TMI, AMSR-E, and SSM/I are converted to precipitation estimates at the TRMM Science Data and Information System (TSDIS) with sensor-specific versions of the Goddard Profiling Algorithm (GPROF). GPROF is a physically- based algorithm that attempts to reconstruct the observed radiances for each FOV by selecting the “best” combination of thousands of numerical model generated microwave channel upwelling radiances, [6]. The associated vertical profiles of hydrometeors are used to provide an estimated surface precipitation rate. The microwave data are screened for contamination by surface effects as part of the processing, with marginal contamination denoted as “ambiguous.” Passive microwave FOVs from AMSU-B are converted to precipitation estimates at the National Environmental Satellite, Data, and Information Service (NESDIS) with operational versions of the algorithm by [9].

The TMI—AMSR-E and TMI—AMSU-B calibrations are set in the form of a single climatological adjustment for land and ocean applications. The rainfall estimates are calibrated for each satellite and audited for >40% "ambiguous pixels". Individual grids are p opulated by the "best" data from all available overpasses. The most

likely number of overpasses in the 3 hr. window for a given grid box is either one or zero. In the event of multiple overpasses, data from TCI, TCI-adjusted TMI, TCI-adjusted AMSR-E, and TCI-adjusted SSM/I are averaged, and TCI-adjusted AMSU-B estimates are used if none of the others are available for the grid box (Description after [8], [10]).

The research product uses two different IR datasets for creating the complete record of 3- hourly 0.25° grid box histogram is zenith-angle corrected, averaged to a single T_b value for the grid box gridded Tb's. The CPC merged IR is averaged to 0.25° resolution and combined into hourly files as 30 min from the nominal. The result is to provide the high temporal resolution estimate that is typical when satellite data is corrected for small bias by gauge analysis over land. Detailed information on this algorithm is available at the link: http://pps.gsfc.nasa.gov/tsdis/Documents/ICSVol4.pdf.

In [5] it is described that TMPA provides reasonable performance at monthly scales. It is further described that TRMM TMPA data has strong physical relationship to the hydrometeors that result in surface precipitation although it is shown to have some error due to lack of sensitivity to low precipitation rates over ocean in one of the input products namely AMSU-B. Other aspects that affect performance are that each individual satellite provides sparse sampling by course space resolutions so occurrence of precipitation is relatively poorly represented. In addition there are significant gaps in the current 3-hourly coverage by the passive microwave estimates even when images are combined and merged to improve spatial coverage (after [8]). Performance assessments of the TRMM 3B42 satellite rainfall product in the Cuvelai basin that stretches from Angola to Namibia are not known to the authors. Lack of verification is caused by the lack of in-situ measurements and, as such, products must be considered uncertain. The product 3B42 v6 is available from GIOVANNI TOVAS in four formats: HDF, NetCDF (NCD), ASCII (available only when the array size is within about half-million points), and Google Earth KMZ.

2.3 LSA-SAF Evapotranspiration (ET)

The evapotranspiration (ET) product is derived from EUMETSAT Land Surface Analysis Satellite Application Facility (LSA SAF). Two products from the EVIRI radiometer on board the MSG satellite are produced. These are the instantaneous ET (30 minutes) and the daily ET both at spatial resolution of 3 km^2. The ET algorithm targets the quantification of the flux of water vapor from the ground surface (soil and canopy) into the atmosphere using input data derived from Meteosat Second Generation (MSG) satellite. The product used for Cuvelai basin was taken from Southern Africa (SAFr) geographical area with in the Meteosat disk, covering the African continent south of the equator. Figure 2 shows evapotranspiration estimated for 11th February 2009. Detailed information on the ET product is available at the following link: http://landsaf.meteo.pt.

The procedure follows a physically based approach which can be described as a combination of the Soil-Vegetation-Atmosphere Transfer (SVAT) scheme and Tiled Land-Surface Scheme (TESSEL) land surface model. To simplify the estimation, the SVAT scheme is modified to read satellite remote sensing derived data combined with data from numerical weather prediction (NWP) as forcing. Detailed information on the TESSEL model is available at: http://www.ecmwf.int/research/EU_projects/GEOLAND/CTESSEL/index.html. The TESSEL land surface model is a physically based model with specific algorithms for e.g. snow, soil moisture and runoff (we refer to [11] for further descriptions). Subject to the application, the model often uses MSG images as input. In the approach each pixel is considered a "mosaic" [11] of tiles representing a particular coverage type (bare soil, grassland, crops, and forests). Some parameters are defined at the pixel level and are thus shared by the tiles composing the pixel, while others are defined at tile level (i.e. overlay by a single tile), most of them being extracted from the ECOCLIMAP database [12]. Masson *et al.* 2003). The resulting ET estimate for each pixel is obtained through the weighted contribution of each considered tile in the pixel [Description after [11].

2.4 GLOBCOVER land-use map

The land use map of Cuvelai basin was extracted from the GLOBCOVER global map, at a spatial resolution of 300 meters. The GLOBCOVER project was launched in 2004 as an initiative of ESA. It has now evolved to an international collaboration between ESA, FAO, UNEP, JRC, IGBP and GOFC-GOLD. The objective of GLOBCOVER is to produce a global land-cover map for the year 2005 at high resolution (300 m × 300 m) using data from MERIS sensor on-board ENVISAT satellite.

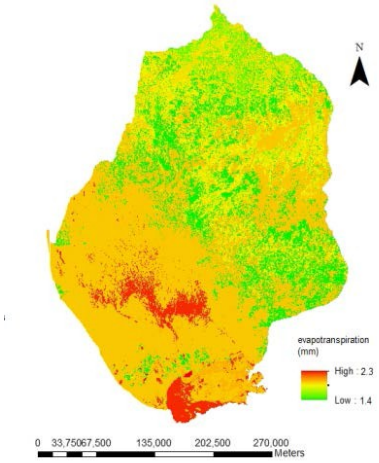

Figure 2: Evapotranspiration estimate 11th febr.2009.

The GLOBCOVER product intends to complement and update other existing comparable global products, such as the global land cover map for the year 2000 with a resolution of 1 km × 1 km produced by the JRC. Appropriate approaches for the validation of the land cover products are planned to be defined in consultation with Centre for Earth Observation Science (CEOS). Details of the GLOBAL cover map are available from http://geoserver.isciences.com:8080/geonetwork/srv/en/metadata.show?id=228. Figure 3 show maps of the Cuvelai area as available through GLOBCOVER and reprocessed following the classification of the CoRINE data base. The newly created land use polygon dataset was reclassified from the GLOBCOVER land cover classes to match the land cover classification of the CoRINE data base (http://www.ceh.ac.uk/data/LCM1990Categories.html) used by LISFLOOD.

MODIS Leaf Area Index

LAI is an important input for the LISFLOOD model, since it is used as in put to estimate interception, evaporation of intercepted water, evapotranspiration and evaporation from the soil surface. For this study we used the MODIS product that is available at https://lpdaac.usgs.gov/lpdaac/products/modis_products_table. The product algorithm uses sun and view angle directions of the MODIS satellite to estimate LAI values based on Bidirectional Reflectance Factor (BRF) for each MODIS band, band uncertainties, and six biomass land cover classes, [13]. Images are available at daily basis.

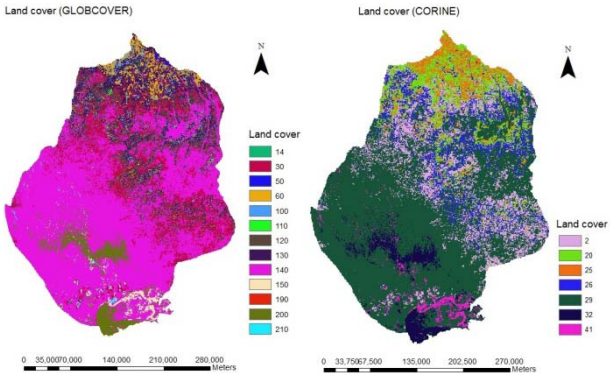

Figure 3: CoRINE land cover classes and GLOBCOVER land cover classes

The processing is done by NASA and daily LAI values are composited over an eight day period. The products are distributed from the EDC Data Center as 1 km 8-day products. Figure 4 shows LAI of the Cuvelai area for the 9th of 2009. Note that LAI changes over time depending on crop growth stages and soil water availability.

For this pilot study we used averaged LAI at monthly base. Since each satellite product is affected by aspects that relate to the specific sensor technology, time-space resolution, sub-grid variability, satellite observation algorithm and its specific parameters (just to mention a few) each product must be asse ssed for its accuracy. Table 2 reports on the quality aspects and assessments performed on the satellite products.

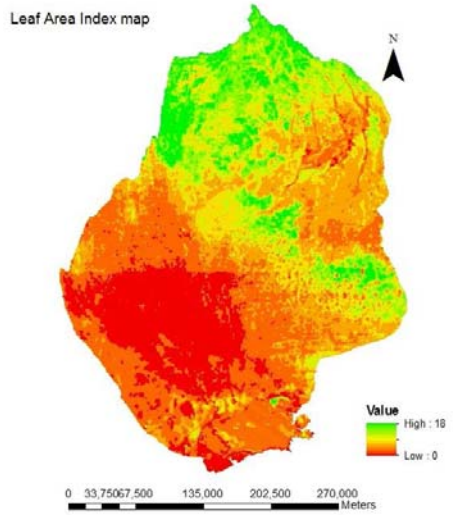

Figure 4: Leaf Area Index map of the Cuvelai area (24 February 2009).

Table 2: Quality assessment of satellite data

Satellite imagery	Quality assurance / accuracy levels
SRTM DEM	The SRTM DEM has an average error of 8 m as opposed to 20 m for the TOPO DEM. In area specific studies around the world systematic errors were identified in the SRTM data, related to aspect. The errors were found to be highest in northeast-facing slopes, attributed to the effect of incidence angle of the original radar images used to produce the SRTM DEM. http://srtm.csi.cgiar.org/PDF/Jarvis4.pdf
Precipitation TRMM 3B42	v6-All TRMM products are provided with random error estimates. The data record have gaps in the record due to processing errors and down time on receivers related to satellite imagery shortcomings. TMI error detection and correction is done by deleting all pixels with non- physical Tb and local calibration errors. ftp://precip.gsfc.nasa.gov/pub/trmmdocs/3B42_3B43_doc.pdf
Evapo-transpiration (ET)	The error estimate is the most general quality indicator operationally delivered by the algorithm. Automatic quality control (QC) is performed on each product and the quality information is provided on a pixel basis. Dark pixels (uncertainty < 0.1), green (uncertainty 0.1- 0.15), yellow pixels (uncertainty 0.15 - 0.20), red pixels correspond to unusable areas. http://www.earsel.org/symposia/2009-symposium- Chania/09EARSEL_garciaharoetal_LSASAF.pdf
MODIS Leaf Area Index	Science data quality flag was inferred as 'passed'on 17/04/2002, but the following is to be observed: Over inland water bodies (rivers, lakes, etc...) surface reflectance inputs and VI values are not stable and should be used with caution. Users are advised to examine the per-pixel product quality to screen poor data before applying it to project-applications, science, and research. http://landweb.nascom.nasa.gov.
GLOBECOVER Land use	The final product has a relative RMSE of <50 mand <80 m absolute RMSE. Corrections have been implemented to diminish the influence of the atmosphere.In order to minimise the bi-directional reflectance effects a simple composition averaging (BRDF correction) was used. http://due.esrin.esa.int/prjs/Results/20110202183257.pdf
Land surface temperature (LST) (LST only serves snowmelt calculations	Errors in the data such include individual pixel count errors, missing parts of scan-lines, wrong geo-location and missing periods. There are also unknown errors in ECMWF re-analysis http://postel.mediasfrance.org/IMG/pdf/CSP-0350-ATBD_LST- I1.00.pdf

3 Hydrological modeling

For this study the LISFLOOD model was selected that serves for large scale stream flow and inundation modeling. LISFLOOD is a spatially distributed and physically-based hydrological model [14], [15]. The model simulates river discharge in a drainage basin as a function of topography, model forcing data, soil properties and land cover. The primary output of the model is the stream flow (i.e., channel flow discharge). Other outputs are the internal flux rates and state variables. For the LISFLOOD training version that was received from the JRC only the streamflow output was activated so time series on internal states and flood inundation were not available for the simulation period.

All output can be written as grids, or time series at user-defined scales, points or areas. The structure of the LISFLOOD can be characterized as follows [16]:

a) 2-layer soil sub-model for shallow subsurface flow
b) sub-models for groundwater and sub-surface flow
c) a sub-model for the routing of surface runoff
d) a sub-model for the routing of stream flow.

The processes simulated by LISFLOOD are precipitation, interception, soil freezing, snow melt, infiltration, percolation, capillary rise, ground water flow and surface runoff. Surface runoff and channel routing are routed separately using a GIS based kinematic wave routing module as the Manning equation, [16]. All satellite products used in this study that served as inputs are described in Section 2. Below a short description is added on the non-satellite model inputs.

Non-satellite based model inputs

Soils

By its physical base, for simulation of the soil moisture storage and movements of the unsaturated zone, the LISFLOOD model uses a so called "Richards type" flow equation. This equation is parameterized by the, so called, "van Genuchten" relations which calculates soil moisture based on saturated volumetric soil moisture content (θ_s), residual volumetric soil moisture content (θ_r), a pore size index (λ) , saturated conductivity (K_s) and the Van Genuchten parameter Alpha (α). For each of these parameters values need to be defined that reflects on the actual soils in the study area.

Table 3: Soil texture at 1m depth (Hor. A)

	θ_s	θ_r	λ	α	K_s [cm/d]
Acrisol	0.439	0.01	0.1804	0.0314	2.061
Chernozem	0.52	0.01	0.1012	0.0367	24.8
Luvisols	0.403	0.025	0.3774	0.0383	60
Solonchacks	0.614	0.01	0.1033	0.0265	15
Solonets	0.430	0.01	0.2539	0.0083	2.272

(Source: Rawls *et, al.* 1982) ([17])

The project area was extracted from the regional soils map of Africa using the Cuvelai basin boundary file 'Cuvelai.shp' created in the ArcMAP spatial analyst tools. The vector-based soils data files were then reclassified from the FAO/UNESCO classes to match the LISFLOOD-USGS classes for which related tables are available in the LISFLOOD manual. Soil parameters are linked to the soil texture and land use maps through look-up tables. The LISFLOOD model requires soil depth and soil texture to be defined for two horizons

Channels

For transfer of runoff water to the basin outlet, a Strahler order drainage network is used. The network evolves from upstream element mapping. Runoff from any grid element is simulated based on a kinematic wave approximation and requires that channels need to be parameterized at pixel level. In this study fixed properties are defined for each respective Strahler order. In this study channel properties such as bank width, bank height, dimensions for the respective Strahler orders increase from upstream to the downstream with largest values at the outlet. A major constrain to this approach in the Cuvelai area in Namibia is that flow behavior in the Oshannas cannot be simulated accurately and reliably by issues of spatial scale and data availability. For instance, the DEM resolution (5 km × 5 km) is much to course to represent conveyance characteristics of the Oshannas.

Stream flow measurements

For this study, stream flow data was not available and constrained model calibration. To overcome this problem information on water levels from TerraSar maps was used and stream flow was estimated by considering the (total) accumulated cross-sectional area of the Oshannas that drain the water. Clearly, this procedure must be considered 'rudimentary' and results of estimated stream flow must be considered very inaccurate and thus unreliable. Results of the inversely established stream flow hydrograph are shown in the section on model calibration.

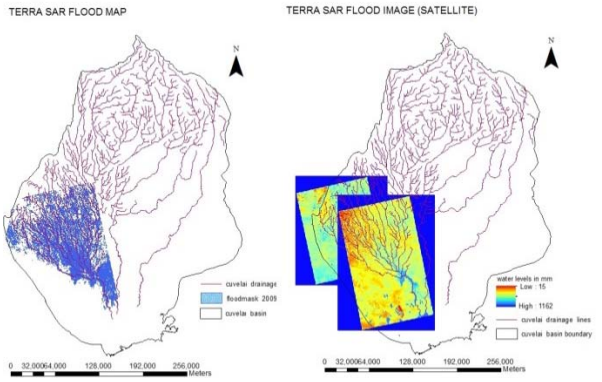

Figure 5: Cuvelai drainage network overlain by TerraSar flood maps.

4 Modeling results

Outputs by LISFLOOD are generated as PCRaster maps of as time series. In the LISFLOOD model version applied for this study the flood inundation mapping was inactive and focus only was on large scale stream flow modeling. Moreover, the course grid element scale adapted in this study (5 km × 5 km) did not allow for flood inundation simulation since inundation is at spatial scales much smaller than the pixel foot-print scale. We note that stream flow results from the course scale model could serve as input when setting up a model at fine scale (<100 m^2 resolution).
In this study we simulate the stream flow that caused the flood situation of February-March 2009. Detailed field measurements on flow discharges are not available. This since each Oshanna cannot be equipped with a gauge and since measuring the geometry of each Oshanna is virtually impossible. We estimated stream flow by considering all wetted cross-section on areas of the Oshannas that contributed to the conveyance of the water. Since the Cuvelai area in Namibia is very flat, much runoff water is stored and very small hydraulic gradients drive the flow of water. As such the stream flow estimates must be considered very uncertain.

The model was initialized using a period of 1000 days. Since data only was available for the wet season period in 2009 we repeated simulations where output of all state variables served as input for the next simulation run. By the sequence of simulation runs we assume that the model is initialized. The model initialization run is shown in figure 6. The actual simulation period during which floods occurred stretches from 21st January to 28th February.

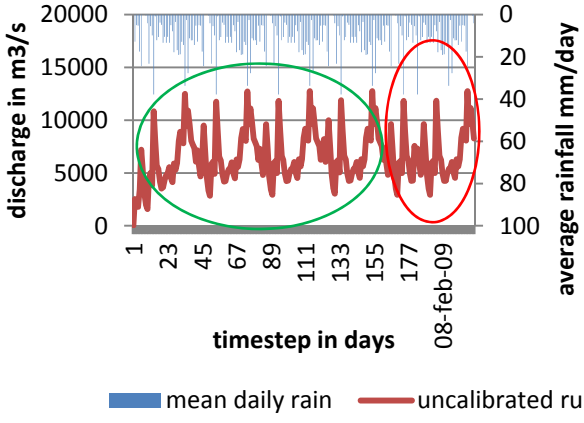

Figure 6: Model simulated discharge against rainfall received

It is shown that timing of the peaks of the discharge from the period of interest marked in the red circle does not directly correspond to the rainfall received. Thus calibration of the model was carried out to improve timing of the peak flows with the maximum average daily rainfall received. Calibration was based on a sensitivity analysis for five parameters suggested by [18]. Parameters and their calibrated values are: two infiltration parameters *b_Xinanjiang* (0.8) and *PowerPrefFlow* (5) as well as *UpperZoneTimeConstant* (15) that is a time constant for the upper groundwater zone [days]; the *LowerZoneTimeConstant* (2500), a time constant for the lower zone in days and *GwPercValues* (1.2), the maximum rate of percolation going from the upper to lower groundwater zone (mm/day).

Figure 7 shows results of two stream simulation runs from this study and inversely estimated stream flow from the flood estim ates. Graphs indicate that discharge estimations inferred from the flood maps are reasonably simulated by the model. This applies for the simulations that apply optimized model parameters (i.e., calibrated) but also default parameters (i.e., default). Both simulation results, however, generate lower flows over the simulation period suggesting that the estimated flow discharges are too high. With respect to timing of peak flows, results when using calibrated parameters shows a better match. Performance indicators suggest fair model performance with relatively low NS values (0.59) and high RMSE values (83 m^3/s). Overall it can be stated that the model shows potential to be applied to the Cuvelai with satellite products that serve for meteorological model forcing.

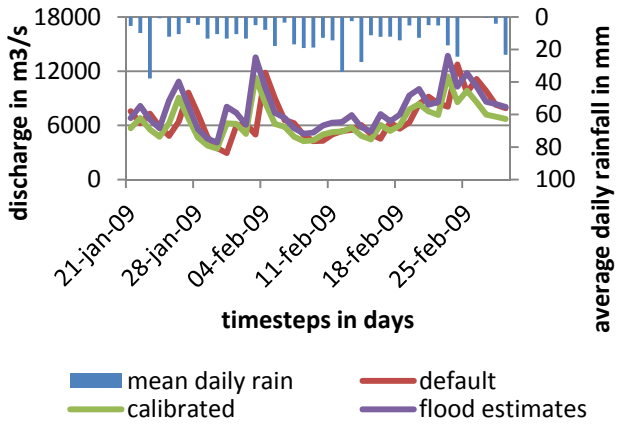

Figure 7: Simulated streamflow.

5 Discussion and Conclusions

The general conclusion is that it is possible to simulate flood events in large, data scarce, catchments using the LISFLOOD model and a number of satellite products. The hydro-meteorological satellite data selected for this study proved to be useful to force the model. Also representation of topography, land use and leaf area index by satellite data seems to be appropriate although specific (validation) assessments on the products could not be performed by lack of field data.

Model sensitivity analysis indicates that the model is very sensitive to the parameter *b_Xinanjiang*. Peak flows as well as flows during inter-storm periods are affected although we did not perform volumetric tests on the total discharged water. The LZTC controls slow runoff contributions to stream flow. LZTC also affects 'timing' of the peaks and shows a shift towards better coincidence with rainfall events. The UZTC is the least sensitive of the parameters, and generally any values within the suggested range can be used within the context of this study and with the dataset available because from a minimum of 10 to a maximum of 50 the response is a lmost negligible. The channel bottom width and the channel bankfull maps are critical to the accurate simulation of water levels through kinematic routing.

Very poor availability of in-situ data caused that simulation results are very uncertain. Stream flow estimates from the Cuvelai in Namibia only are inversely estimated. This by considering the conveance area of the Oshannas. We note that estimates during inter-storm periods and peak flows cannot be reasoned for when compared to observed flows from catchments of similar size. Measurements by the Ministry of Agriculture, Water and Forestry in Namibia suggest flows as small as 200 to 300 m^3/sec. Discharges of this magnitude, however, commonly are observed at catchments of maximum regional scale (1500 km^2). We speculate that most runoff water is stored in the Oshannas in the very flat Cuvelai area at the Angolan-Namibian border causing inundation and the low discharge. Since flat areas are characterized by (very) small hydraulic gradients, this could explain why flow estimates are of different magnitude. Clearly, hydraulic behavior should be evaluated and substantiated by field assessments and verification.

Acknowledgements

This study is supported by the European Space Agency (ESA) through the ESA-TIGER capacity building initiative in Africa and refer to http://www.tiger.esa.int/page_training.php. The study is also supported by Twente University, Faculty of Geo-Information Science and Earth Observation (ITC) and the Ministry of Agriculture, Water and Forestry in Namibia.

Reference

1. DWAF (2010). "Rural water developing and planning." Retrieved 17 August 2010, from http://www.mawf.gov.na/Directorates/RuralWaterSupply/support.html.
2. NHS (2010, 17 August 2010). "Flood report archives." Retrieved 29 August 2010, from http://www.mawf.gov.na/index.html
3. Farr, T., G and M. Kobrick (2000).The Shuttle Radar Topography Mapper.NASACenter. J. P. Laboratory. USA. 200 10012851.
4. USGS (2006).Shuttle Radar Topography Mission.College Park, Maryland, Global Land Cover Facility, University of Maryland.
5. Huffman, G.J., R.F. Adler, D.T. Bolvin, G. Gu, E.J. Nelkin, K.P. Bowman, Y. Hong, E.F. Stocker. (2007). The TRMM Multi-satellite Precipitation Analysis: Quasi-Global, Multi-Year, Combined-Sensor Precipitation Estimates at Fine Scale. J. Hydrometeor., 8(1), 38-55.
6. Huffman, G.J., R.F. Adler, B. Rudolph, U. Schneider, and P. Keehn, 1995: G lobal Precipitation Estimates Based on a Technique for Combining Satellite-Based Estimates, Rain Gauge Analysis, and NWP Model Precipitation Information, *Journal of Climatology.*, 8, 1284-1295.
7. Xie, P. and P. A. Arkin (1997)."A 17 year monthly analysis based on gauge observations, satellite estimates, and numerical model outputs. "Bulletin of American Meteorological Society 78 (11): 2539-2558.
8. Huffman, G.J., and Bolvin, D.T., (2013) TRMM and Other Data Precipitation Data Set Documentation. http://precip.gsfc.nasa.gov/trmm_comb.html
9. Weng, F. and Q. Liu, 2003: Satellite data assimilation in numerical weather prediction models, 1. Forward radiative transfer and Jacobian models under cloudy conditions, *J. Atmos. Sci.*, **60**, 2633 - 2646.
10. Acker, J. G., and G. Leptoukh (2007), Online analysis enhances use of NASA Earth science data, Eos Trans. AGU, 88 (2), 14
11. Gellens-Meulenberghs, F.; Arboleda, A and Ghilain, N. , (2007) Towards a continuous monitoring of evapotranspiration based on MSG data. Accepted contribution to the proceedings symposium on Remote sensing for environmental monitoring and change detection. IAHS series. IUGG, Perugia , Italy
12. Masson, V.; Champeaux, J. L.; Chauvin, F.; Meriguet, C.; Lacaze, R. A. (2003). Global database of land surface parameters at 1km resolution in meteorological and climate models. Journal of Climate 16(9), 1261-1282

13. Ranga, M.; Steven, W.; Running, J.; Glassy, P. (2000) User's Guide FPAR, LAI (ESDT: MOD15A2) 8-day Composite NASA MODIS Land Algorithm (Doc v1.0-09.14-jmg).

14. De Roo, A.P.J., L. Hazelhoff and P.A. Burrough 1989. 'Soil erosion modeling using 'ANSWERS' and Geographical Information Systems'. Earth Surface Processes and Landforms, 14, 517-532.

15. De Roo, A.P.J. 1996 'Soil Erosion Assessment Using GIS.' In: Singh, V.P. and Fiorentino, M. (eds.) Geographical Information Systems in Hydrology. Kluwer. 443 p.

16. De Roo, A. P. J. , Wesseling, C. G. and Van Deursen, W. P. A. (2000) Physically based river basin modeling within a GIS: The LISFLOOD model.. Hydrological Processes 14 , pp. 1981-1992.

17. Rawls, W., D. Brakensiek, et al. (1982). "Estimation of Soil Water Properties" American Society of Agricultural Engineers 25.

18. Van der Knijff, J. and A. De Roo (2008). LISFLOOD Distributed Water Balance and Flood Simulation Model. Revised User Manual. Luxembourg, Joint Research Centre, European Commission. ISSN 1018-5593.